Journal of Environmental Management 292 (2021) 112737

Contents lists available at ScienceDirect

Journal of Environmental Management

journal homepage: www.elsevier.com/locate/jenvman

Research article

Response of European grayling, *Thymallus thymallus*, to multiple stressors in hydropeaking rivers

Daniel S. Hayes [a,b,*], Erwin Lautsch [b], Günther Unfer [b], Franz Greimel [b], Bernhard Zeiringer [b], Norbert Höller [c], Stefan Schmutz [b]

[a] Forest Research Center, Instituto Superior de Agronomia, University of Lisbon, Portugal
[b] Institute of Hydrobiology and Aquatic Ecosystem Management, University of Natural Resources and Life Sciences, Vienna, Austria
[c] Center for IT Services, University of Natural Resources and Life Sciences, Vienna, Austria

ARTICLE INFO

Keywords:
Classification and regression tree
Configuration frequency analysis
Hydro-morphology
Hydropower
Salmonidae
Sub-daily flow fluctuations

ABSTRACT

Rivers of the large Alpine valleys constitute iconic ecosystems that are highly threatened by multiple anthropogenic stressors. This stressor mix, however, makes it difficult to develop and refine conservation and restoration strategies. It is, therefore, urgent to acquire more detailed knowledge on the consequences and interactions of prevalent stressors on fish populations, in particular, on indicator species such as the European grayling *Thymallus thymallus*. Here, we conducted a multi-river, multi-stressor investigation to analyze the population status of grayling. Using explorative decision-tree approaches, we disentangled the main and interaction effects of four prevalent stressor groups: flow modification (i.e., hydropeaking), channelization, fragmentation, and water quality alteration. Moreover, using a modified variant of the bootstrapping method, pooled bootstrapping, we determined the optimal number of characteristics that adequately describe fish population status. In our dataset, hydropeaking had the strongest single effect on grayling populations. Grayling biomass at hydrological control sites was around eight times higher than at sites affected by hydropeaking. The primary parameters for predicting population status were downramping rate and peak amplitude, with critical ranges of 0.2–0.4 cm min^{-1} and 10–25 cm. In hydropeaking rivers, river morphology and connectivity were the preceding subordinated parameters. Repeating the procedure with pooled bootstrapping datasets strengthened the hypothesis that the identified parameters are most relevant in predicting grayling population status. Hence, hydropeaking mitigation based on ecological thresholds is key to protect and restore already threatened grayling populations. In hydropeaking rivers, high river network connectivity and heterogenous habitat features can dampen the adverse effects of pulsed-flow releases by offering shelter and habitats for all life cycle stages of fish. The presented approach of explorative tree analysis followed by post-hoc tests of identified effects, as well as the pooled bootstrapping method, offers a simple framework for researchers and managers to analyze multi-factorial datasets and draw solid management conclusions.

1. Introduction

The European grayling *Thymallus thymallus* is an indicator species for the ecological integrity of an entire river region – the grayling zone, which encompasses rivers in wide mountain valleys (Huet, 1959). Unfortunately, grayling stocks in Europe have plummeted in the last decades, underlining the urgency of conservation measures targeted at this species and fish region (e.g., Müller et al., 2018). However, it remains challenging to establish the most effective management and restoration strategies as rivers of the grayling zone, also called hyporhithral rivers, are often impacted by multiple anthropogenic stressors such as river regulation, connectivity disruption, and channelization (Schinegger et al., 2012). In the European Alps alone, 80% of all larger rivers with a catchment size of >500 km^2 are affected by diverse hydromorphological impacts (Muhar et al., 2019).

Of these impacts, the effects of storage hydropower plants are particularly prevalent in hyporhithral rivers (Fig. 1). Storage hydropower plants are run according to energy demand, thereby causing artificial (sub-daily) flow fluctuations by the discontinuous release of turbined water (Greimel et al., 2016). Such water releases, called

* Corresponding author. Forest Research Center, Instituto Superior de Agronomia, University of Lisbon, Portugal.
E-mail address: daniel.hayes@boku.ac.at (D.S. Hayes).

https://doi.org/10.1016/j.jenvman.2021.112737
Received 26 January 2021; Received in revised form 28 April 2021; Accepted 29 April 2021
Available online 12 May 2021

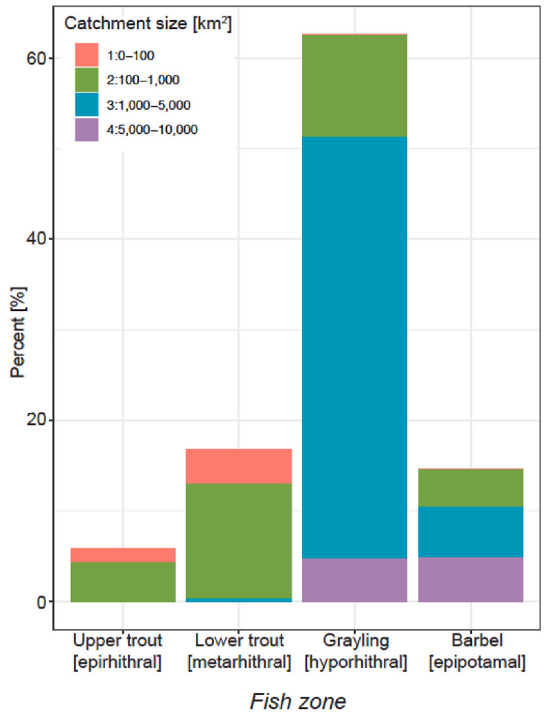

Fig. 1. Hydropeaking rivers in Austria according to fish region and catchment size (data source: BMLFUW, 2017).

hydropeaking, have wide-ranging implications for river ecosystems. Hydropeaking can influence spawning activities and behavior, or cause drift and stranding of juvenile fish as well as of aquatic insects, thereby reducing recruitment rates and food supply (Greimel et al., 2018; Hayes et al., 2019). Unsurprisingly, in Austria, of the almost 900 river kilometers labeled as hydropeaking-impacted, 82% are in risk of failing the objectives of the EU Water Framework Directive (BMLFUW, 2017). However, considering that also run-of-river hydropower schemes can cause hydropeaking (though usually of lower intensity) (Greimel et al., 2016), it is likely that the threat of failing to achieve ecological objectives due to hydropeaking is even higher than initially perceived.

Another common stressor is morphological riverbed degradation caused by river engineering works (Schinegger et al., 2012). As widely known, river straightening and bank stabilization decrease suitable habitats, particularly shallow shoreline areas needed for the rearing of juvenile fish (Jungwirth et al., 2000). Considering that <20% of Austrian grayling rivers still exhibit good habitat quality (Muhar et al., 2000), it can be expected that this trend is reflected in fish population status.

Moreover, river engineering and hydropower development have not only channelized but also fragmented most of the world's rivers (Grill et al., 2015). Instream connectivity, however, plays a fundamental role for life cycle completion of many fish species. The grayling, a medium-distance migratory species, requires an open river corridor for spawning migrations but also for movements between summer and winter habitats, as well as distinctive habitat shifts related to early ontogenetic development (Nykänen, 2004; Sempeski and Gaudin, 1995). Although fish passes are nowadays increasingly retrofitted to dams and weirs, they may still cause delayed or insufficient passage or exhibit other drawbacks (Linløkken, 1993; Silva et al., 2018). Moreover, fish may be injured or killed by turbine passage, which is a common route for downstream migration (Harrison et al., 2019). Also, reservoirs may act "as an ecological barrier to downstream movement" (Silva et al., 2018). Hence, highly fragmented river systems may be restricted in supporting vital fish populations.

Many rivers are also affected by alterations of water quality and nutrient content (Schinegger et al., 2012). Grayling populations can respond negatively to deterioration of water quality, and water quality and nutrient baseline conditions such as saprobity are known to influence fish distribution (Vannote et al., 1980).

Overall, it is apparent that grayling populations are affected by multiple stressors (Muhar et al., 2007). As stressors can override or interact with each other, it remains challenging to define the best river management approaches. To develop and refine conservation and restoration strategies, it is urgent to acquire more detailed knowledge on the consequences and interactions of prevalent stressors on fish populations.

We hypothesized that hydropeaking intensity is the strongest stressor for grayling, followed by river morphology. To test this assumption, we conducted a multi-river, multi-stressor investigation to analyze the population status of grayling in Austria. Although it is common for such approaches that data are sampled in several rivers and over multiple years, this fact makes it difficult to apply inferential statistics. This raises the question of which methodological approach can deal with these preconditions as well as solve the frequent challenge of a comparably small base sample size. In this study, we used explorative methods to identify essential parameters and to elucidate the optimal number of characteristics that adequately describe the status of grayling populations. Thereby, we enhance ecological knowledge to aid river management in establishing the most effective measures for protecting and restoring already threatened grayling populations. Moreover, we offer a simple approach to analyze multi-factorial datasets encompassing sites from different rivers.

2. Materials and methods

2.1. Study area

Fish samples were collected from Austrian hyporhithral rivers where the grayling, according to the national fish catalog, is classified as being a dominant ('Leitart') or accompanying (subdominant) species (BAW, 2007). This classification of the national fish catalog is based on environmental parameters such as bioregion, altitude and catchment size, or historical sources. Regarding flow modifications, our sites ranged from hydrological control sites that are not impacted by hydropower operations to sites of low-intensity hydropeaking ('hydro-fibrillation') and high-intensity hydropeaking (Fig. 2; Greimel et al., 2016). Similarly, our sites also exhibited a strong stressor gradient regarding other impacts.

2.2. Fish stock assessments

Fish data were provided by the Austrian Ministry of Sustainability and Tourism, which we complemented by further field samples. The collection of fish data followed the standard protocol of the national sampling guideline (Haunschmid et al., 2006) under the requirements of the EU Water Framework Directive (2000/60/EC). In short, fish sampling was conducted via electrofishing during low flow conditions in fall. Depending on river size, the fishing campaigns were done by wading, boat, or a mix of both. In smaller rivers, a representative stretch (at least ten times the average river width) was sampled with a two- or three-pass removal approach (DeLury, 1947; Seber and Le Cren, 1967). In larger rivers, habitats were proportionally sub-sampled using electrofishing boats equipped with a boom of anodes (width of operation: 6 m; effective depth: ca. 2.5 m; Schmutz et al., 2001). Fish stocks were calculated as biomass and frequency per hectare based on the sampled area. The reader is referred to Schmutz et al. (2015) for details.

We used grayling biomass per hectare [kg ha^{-1}] to assess the status of grayling populations, as biomass is a robust measure to detect cumulative, multi-annual impacts of a variety of stressors. This target variable (Y_i) is a ratio-scaled variable following a non-parametric distribution.

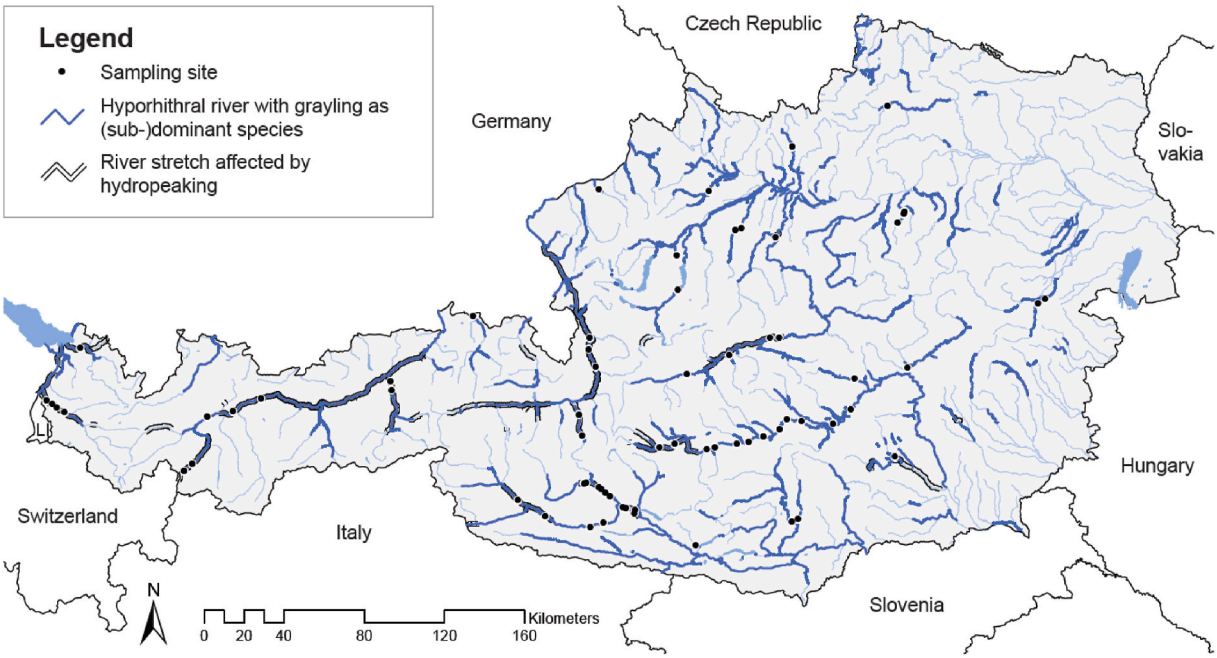

Fig. 2. Hyporhithral rivers of Austria where grayling is a dominant or subdominant species (BAW, 2007), river stretches affected by hydropeaking (BMLFUW, 2017), and fish sampling locations.

2.3. Hydrological features

The Austrian Hydrographic Service provided flow data with a time resolution of 15 min. To quantify hydropeaking events, we assessed ecologically-relevant event-based parameters (see Table 1) according to Greimel et al. (2016, 2017). The statistical characteristics were calculated out of five years prior to each fish survey to match flow conditions before and during biological assessments (Schmutz et al., 2015). As variables of increase and decrease event types have proven to be highly redundant (Greimel et al., 2016) we continued working with decrease events only as these are considered being of higher relevance for fish ecological research (Moreira et al., 2019).

We assigned fish sampling stretches to the nearest gauging station that is representative of the hydrological conditions at the sampling site (average distance: 4.1 km). We removed all sites that did not have relevant gauges and those situated in impoundments or residual flow sections, and those with spatial autocorrelation issues with other sites, thereby reducing the number of sites from 197 to 69.

Table 1
Overview of parameters.

Stressor block[a]	Parameter	Abbreviation	Unit
H	Yearly number of events[b]	CNT	n
	Yearly number of daytime events[b]	CNT_D	n
	Yearly number of nighttime events[b]	CNT_N	n
	Peak amplitude[c]	AMP_dW	cm
	Duration[b]	DUR	min
	Base/peak flow ratio[b]	RATIO	
	Mean downramping rate[b,c]	MEFR_dW	cm min^{-1}
	Maximum downramping rate[b,c]	MAFR_dW	cm min^{-1}
M	Channel width index	CW	
	Standard sinuosity index	SSI	
C	Habitat connectivity index 1[d]	CONN_1	km
	Habitat connectivity index 2[d]	CONN_2	km
Q	Biological assessment: pollutant load	POLL	[ordinal]
	Saprobity baseline status	SAP	[ordinal]

[a] H = hydropeaking, M = morphology, C = river connectivity, Q = water quality.

[b] Ecologically-relevant event-based flow fluctuation (hydropeaking) parameters following Greimel et al. (2016). To conduct a standardized selection of relevant events out of multiple hydrographs, events of very low intensity regarding up- and downramping rates were excluded (<10% of expected annual natural maximum). All values are means regarding to the selected events.

[c] Parameters describing water level alteration (dW) were transformed into cm or cm min^{-1}. These estimations regarding mean water level conditions are based on a regression model with the input parameters altitude, mean flow conditions, catchment size, and bankfull river width (Greimel et al., 2017).

[d] Indices are based on grayling jump height: 1 = minimum (0.4 m), and 2 = average (0.75 m) jump height (according to Baudoin et al., 2015).

2.4. Morphological features

We assessed a gradient from nature-like to channelized rivers to enhance understanding on the effect of habitat conditions on fish populations in hydropeaking rivers (Schmutz et al., 2015); therefore, we tested two morphological indices based on aerial image interpretation.

The first index, the channel width index, reflects the variability of the channel width in hyporhithral rivers (Greimel et al., 2017). It is based on the coefficient of variation of the active channel width, which is calculated by the ratio between standard deviation and mean. Each fishing stretch was divided into as many 500 m sections needed to cover its entire length. For each 500 m section, we measured ten transects with 50 m distance and calculated the coefficient of variation. If a fish sampling site encompassed multiple 500 m sections, we averaged the interim results to gain an index for the entire stretch. The resulting coefficient allows a comparison of rivers of different dimensions. As a rough guide, sites with a value of <0.1 can be regarded as being heavily channelized. Those with an index between 0.1 and 0.2 are still considered morphological degraded but may feature small-scale widenings or bay structures. Sections with an index >0.2 constitute structurally diverse, nature-like reaches (Greimel et al., 2017).

The second index, the standard sinuosity index, is based on the idea that sinuosity is an effective functional measure of a rivers' morphological status. Also, sinuosity governs the hyporheic patchiness of the stream bed (Braun et al., 2012). The standard sinuosity index is calculated by dividing the channel index (CI) with the valley index (VI). CI is channel length divided by aerial length, and VI is valley length divided

by aerial distance. In general, a straight river has an index <1.05, a sinuous river ranges from 1.05 to 1.3, a moderately meandering one from 1.3 to 1.5, and a meandering river has a sinuosity >1.5 (Horacio, 2014).

2.5. Connectivity features

Habitat fragmentation is considered a crucial factor in influencing species distribution. However, "the effects of fragmentation depend on the size of the resulting fragments" (Fuller et al., 2015). Taking this into account, we calculated the length of the accessible river network between all barriers for each sampling site, whereby we based this calculation on the grayling's natural core distributional area (see Fig. 2). We defined a barrier based on jump heights of grayling, whereby we calculated two habitat connectivity indices: the first was based on the minimum (0.4 m) and the latter on the average (0.75 m) jump height (Baudoin et al., 2015). In each case, we subtracted the length of reservoirs from the resulting river network if it exceeded 1 km in length, as these would not support recruitment.

2.6. Water quality

To evaluate water quality at the sampling sites, we retrieved a cumulative biological assessment regarding pollutant load from the national monitoring program, as well as a status assessments of national and European priority substances (BMLFUW, 2017). The latter two parameters did not show any variation in the dataset (all sites had the 'very good' or 'good' status, respectively); therefore, we excluded them from analyses. To assess nutrient baseline conditions, we integrated saprobic basic state classes as determined by bioregion and altitude (Stubauer and Moog, 2003).

2.7. Model, data, and statistical analyses

In this study, we aimed to find out which parameters (independent variables), as well as which main and interaction effects, make the variation of the biomass level (dependent variable) transparent. Formally, the multi-factorial univariate model can be expressed as:

$$Y_i \Leftarrow \{ H_{ji} ; M_{ki} ; C_{li} ; Q_{mi} \} \quad [1]$$

whereby H, M, C and Q refer to hydrological, morphological, connectivity and water quality parameters, respectively (see Table 1). As described above, we selected sampling sites of different rivers based on fish ecological criteria. To assemble enough sites, sampling spanned a period of multiple years (2005–2014). However, this targeted arbitrary site selection influences the sample character of the data, which do not fulfill the criteria of a representative sample (i.e., selection, structure and number of sites), thereby disqualifying approaches based on inferential statistics. Hence, an explorative-statistical data analysis approach must be implemented.

Here, we used the following two-fold data evaluation strategy. First, we conducted decision tree analysis (CRT) to identify relevant parameters and main and interaction effects (Breiman et al., 1984). Following, we used a two-dimensional frequency analysis, the configuration frequency analysis (CFA) (Von Eye, 2002; Von Eye et al., 2010), to evaluate the statistical significance of the identified effects (global and local). In light of explorative interpretation, the results of the CFA (e.g., p-value) must not be interpreted strictly; instead, they serve as an orientation aid from a hypothesis-generating point of view.

For step 1, the continuously-scaled dependent variable, grayling biomass, was transformed into an ordinally-scaled variable to predict interaction ranges between low, medium, or high biomass situations. Therefore, we followed two approaches: a statistical and an ecological one. For the first, we trichotomized the target variable (i.e., each category contains 33% of the cases; 1: <3.4 kg ha^{-1}, 2: 3.5–19.9 kg ha^{-1}, 3: ≥20 kg ha^{-1}). For the latter, we classified the target variable into three groups according to ecological relevance (1: <10 kg ha^{-1}, 2: 10–39.9 kg ha^{-1}, 3: ≥40 kg ha^{-1}).

Before the tree analyses, to minimize multicollinearity, we removed redundant independent variables by Spearman rank correlation (a measure of monotony) ($|\rho| > 0.8$), whereby we selected inter-correlated descriptors according to potential ecological significance. We then ran the analysis with the remaining variables using the classification and regression tree (SPSS: CRT) method (Breiman et al., 1984), which corresponds to step-by-step bivariate analysis. The CRT method splits the trees based on an internal measure of homogeneity instead of a statistical test procedure. Here, we used a standard measure, the Gini-coefficient, as a splitting criterion (IBM Statistics, 2016). We set a minimum number of 10 and 5 cases for the parent and child node, respectively.

In step 2, we performed exploratory analysis in line with the two-dimensional frequency analysis (CFA: tree nodes *versus* biomass categories) to evaluate which end nodes (interaction pathways) contribute to the model explanation. We tested for global significance through chi-square tests and used Cramér's V to describe the strength of the overall effects on the target variable. To determine local significance, we performed Bonferroni-adjusted cell-residual tests.

Up to now, work was carried out at the level of the base sample where, due to the relatively small sample size ($n = 69$), the possibilities of finding interactions are quickly exhausted. To compensate this disadvantage, we used a modified variant of the bootstrapping simulation. Bootstrapping is an internal resampling method that draws random samples from the base dataset (with replacement) to create a new dataset (National Research Council, 1988). Here, we adapted the bootstrapping method by randomly drawing multiple ($k = 69$) single bootstrap samples of the original dataset (each sample containing the same case number as the base dataset). These single samples were then pooled into one dataset ($n = 69 \times 69 = 4761$). We hypothesized that such cumulative/pooled bootstrapping simulations increase the number of cases while retaining the overall characteristics of the original dataset, having the advantage that the decision trees can be split deeper, thereby allowing the identification of more and longer interaction chains. To explore this hypothesis, we compared the regular bootstrapping method to the pooled variant: First, using the 69 single bootstrap samples, we tested the stability of the base sample results by assessing which variables consistently reappear in the decision trees and in which level. Following, we ran the CRT models with the pooled bootstrapping dataset.

We used a median test to investigate the hypothesis that hydrological control sites had higher grayling biomass than sites impacted by low- or high-intensity hydropeaking. The level of significance was $p < 0.05$. For pair-wise post-hoc tests, significance values were Bonferroni-adjusted. All analyses were performed with IBM SPSS Statistics 24.

3. Results

In total, we analyzed 69 sites from 30 rivers. Among these sites, 12 were classified as 'hydrological control', 21 as 'hydro-fibrillation' (i.e., low-intensity hydropeaking), and 36 as 'hydropeaking'. In the field samples, grayling biomass ranged from 0.0 to 176.4 kg ha^{-1}. We found strong evidence that the three hydrological impact types affect biomass of grayling populations ($p = 0.004$). In detail, hydrological control sites exhibited a significantly higher biomass (mean = 111.6, SD = 51.2 kg ha^{-1}) than hydro-fibrillation (mean = 16.6, SD = 27.1 kg ha^{-1}, $p = 0.001$) or hydropeaking sites (mean = 11.6, SD = 13.5 kg ha^{-1}, $p = 0.003$). On average, grayling biomass at hydrological control sites was eight times higher than at sites affected by hydro-fibrillation or hydropeaking (Fig. 3).

After removing redundant variables, nine variables were left for tree-based exploration (Table S1). Out of the nine variables, two variables were retained in each of the decision trees (Fig. 4a and b). The main and

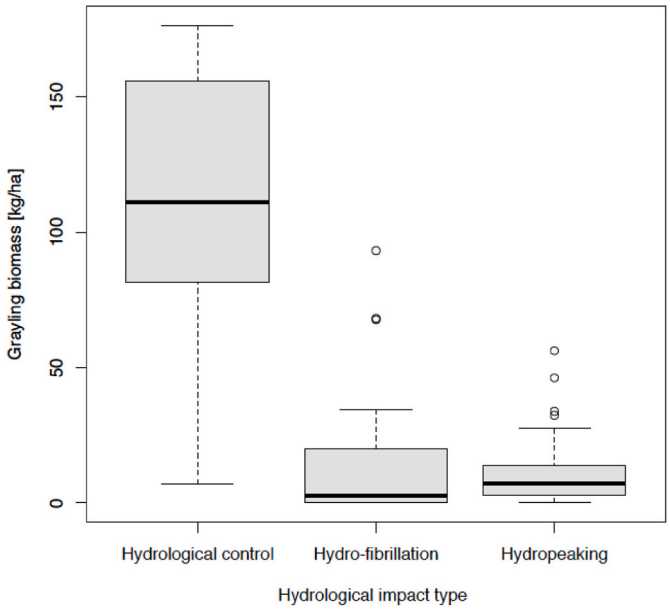

Fig. 3. Grayling biomass at hydrological control sites and those affected by hydro-fibrillation or hydropeaking (grand median = 8.9 kg ha^{-1}). Boxplots: The boxes range from the first to the third quantile, the thick lines represent the median, and the bubbles are outliers (1.5 times the interquartile range).

interaction effects can be explained as follows: The first tree, using the trichotomized target variable, selected mean downramping rate ('MEFR_dW') in the first level as main effect, and habitat connectivity ('CONN_2') in the second level as interaction effect (Fig. 4a). In our dataset, MEFR_dW varies between 0.09 and 1.53 cm min^{-1} (mean = 0.31 cm min^{-1}), and CONN_2 between 0.3 and 177.2 km (mean = 43.7 km) (Fig. S1). The model used MEFR_dW to create the first split: sites with highest biomass had a downramping rate ≤0.18 cm min^{-1}, and those with lower biomass exhibited ramping rates >0.18 cm min^{-1}. These latter sites were split again in the second level using CONN_2 at a threshold of 26.25 km. Sites with low biomass tend to be in more fragmented river reaches, whereas sites with higher biomass are situated within sections of higher connectivity. Overall, the model correctly classified 71.0% of the three biomass categories. In detail, the high and low biomass group performed best (82.6% correct for each group), followed by the medium group (47.8%) (Table S2).

The second tree, taking the ecologically classified variable as dependent variable, yielded a branched pattern similar to the first model but selected peak amplitude ('AMP_dW') in the first level and channel width index ('CW') in the second (Fig. 4b). In our dataset, CW varies between 0.05 and 0.33 (mean = 0.13), spanning a wide range of morphological conditions, and the amplitude of flow fluctuation events varies between 6.5 and 230.5 cm (mean = 32.9) (Fig. S1). For the first split, the decision tree used AMP_dW at a threshold of 10.9 cm to separate higher and lower biomass sites, whereby those with highest biomass showed an amplitude ≤10.9 cm. The other sites (AMP_dW > 10.9 cm) were split again in the second level using CW at a threshold of 0.23, indicating that morphologically impacted reaches are characterized by lower grayling biomass, whereas structurally-diverse river reaches feature higher biomass. Overall, the second model correctly classified 72.5% of the three biomass categories. In detail, the low and high biomass group was correctly classified in 100% and 68.8% of the cases, respectively. The medium biomass groups performed least well with 22.2% correct classification (Table S3).

Following post-hoc tests serve as an orientation aid for the explorative interpretation. Global tests of grayling biomass and the end nodes (interaction pathways) showed a significant influence for both trees (trichotomized: p = 0.000; ecologically classified: p = 0.000; Tables 2 and 3). In both cases, high effect sizes provide security for the model's strength (trichotomized: Cramér's V = 0.597; ecologically classified:

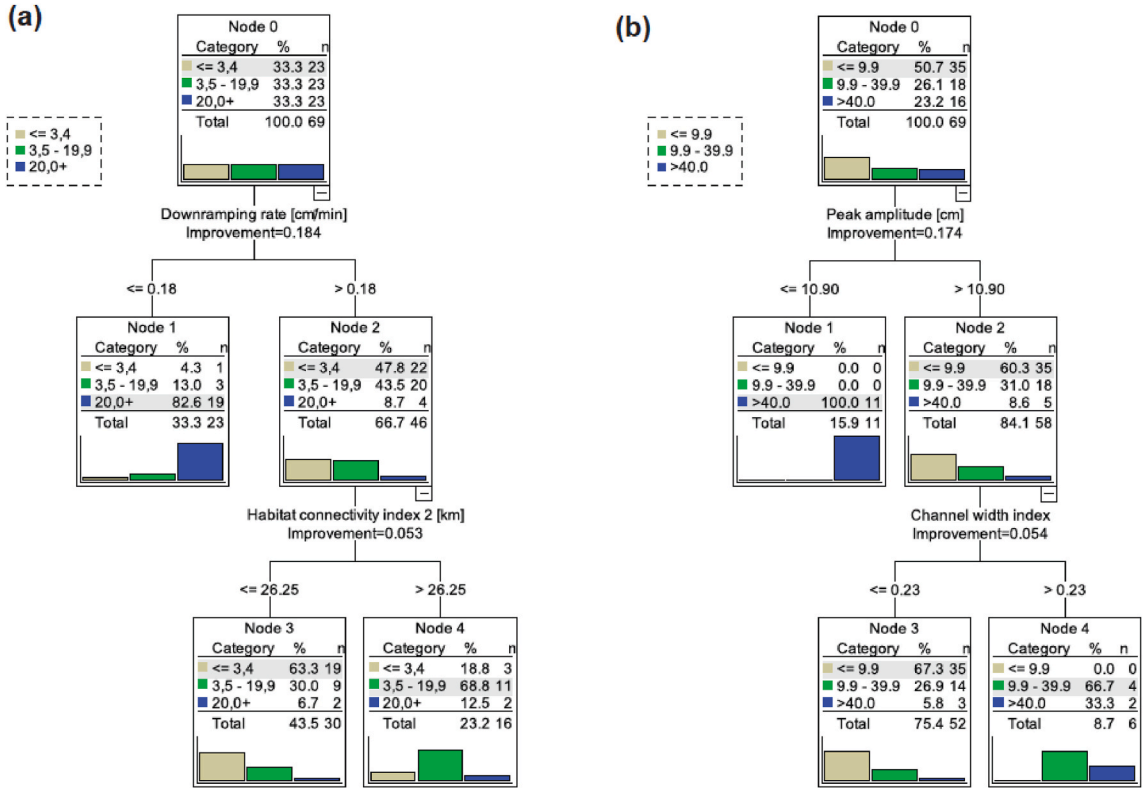

Fig. 4. Explorative decision trees (CRT). (a) Trichotomized target variable; (b) ecologically classified target variable. Both trees show two levels.

Table 2
Cross-table (CFA) results for the end nodes (interaction pathways) versus biomass groups: trichotomization.

Node ID and pathway description		Grayling biomass: trichotomized			
		1: <3.4	2: 3.5–19.9	3: ≥20.0	Total
1: MEFR_dW ≤ 0.18 cm min^{-1}	n	1	3	19	23
	z	**−3.6 (AT)**	−2.5	**6.1 (T)**	
3: MEFR_dW > 0.18 cm min^{-1} & CONN_1 ≤ 26.25 km	n	19	9	2	30
	z	**4.6 (T)**	−0.5	**−4.1 (AT)**	
4: MEFR_dW > 0.18 cm min^{-1} & CONN_1 > 26.25 km	n	3	11	2	16
	z	−1.4	**3.4 (T)**	−2.0	
Total	n	23	23	23	69

Note: Global test results: $CHI^2 = 49.12$, df = 4, p = 0.000; Cramér's V = 0.597. Shown here are observed counts (n) and adjusted residuals (z) to determine typical/overfrequented (T) and atypical/underfrequented (AT) cells. Bonferroni-adjusted level of significance: z $\{\alpha^* = \alpha/\text{frequency of cells} = 0.05/(3 \times 3) = 0.00556\} = 2.77$.

Table 3
Cross-table (CFA) results for the end nodes (interaction pathways) versus biomass groups: ecological classification.

Node ID and pathway description		Grayling biomass: ecologically classified			
		1: <10.0	2: 10.0–39.9	3: ≥40.0	Total
1: AMP_dW ≤ 10.9 cm	N	0	0	11	11
	Z	**−3.7 (AT)**	−2.1	**6.6 (T)**	
3: AMP_dW > 10.9 cm & CW ≤ 0.23	n	35	14	3	52
	z	**4.8 (T)**	0.3	**−6.0 (AT)**	
4: AMP_dW > 10.9 cm & CW > 0.23	n	0	4	2	6
	z	−2.6	2.4	0.6	
Total	n	35	18	16	69

Note: Global test results: $CHI^2 = 53.17$, df = 4, p = 0.000; Cramér's V = 0.621. Shown here are observed counts (n) and adjusted residuals (z) to determine typical/overfrequented (T) and atypical/underfrequented (AT) cells. Bonferroni-adjusted level of significance: z $\{\alpha^* = \alpha/\text{frequency of cells} = 0.05/(3 \times 3) = 0.00556\} = 2.77$.

Cramér's V = 0.621). Extending the test procedure to the performance of local tests highlighted the positioning of the differences. For the first model, five of the nine cells deviated from overall homogeneity (Table 2). In node 1, low biomass sites were underfrequented and high biomass sites overfrequented, whereas the opposite was the case in node 3. In node 4, medium biomass sites were overfrequented. Regarding the second model, we observed local differences for the low and high biomass sites in node 1 and in node 3 – in both cases, the pattern was the same as in the trichotomized model. In node 4, we found no significant differences, even though the low biomass group approached the threshold of statistical significance (Table 3).

Following, we conducted tree analyses with the single bootstrapped samples to assess the frequency of variable occurrence and their location in the tree (Tables 4 and 5). In the trichotomized version trees, the variables MEFR_dW and CONN_2 appeared at the same location as in the base sample in 96% and 44% of the cases, respectively. The trees split into a third level in 52 of 69 cases, with duration ('DUR'), yearly number of peak events ('CNT'), and CW being the dominating variables. Only 38% and 13% of all trees had a fourth and fifth level, respectively (Table 4).

In the ecologically classified trees, the variables AMP_dW and CW appeared at the same location as in the base sample in 61% and 27% of the cases, respectively. MEFR_dW substituted AMP_dW in level one in 36% of the cases but showed a similar split pattern regarding the biomass categories compared to the base sample tree. Variables also frequently occurring in the second level were CNT, AMP_dW, and the standard sinuosity index ('SSI'). In the third level, variable heterogeneity increased, but CNT, CONN_2, and CW were the most frequent parameters. Almost half of the trees did not split beyond the third level, and only 6% reached the fifth level (Table 5).

The pooled bootstrapping approach revealed that the base sample covered the primary effects of levels 1–2. In comparison to the base sample trees, however, the pooled bootstrapping trees produced wider and deeper branching patterns, thereby yielding more end nodes (13 and 10, respectively; Figs: S2-S3).

4. Discussion

Multi-river studies are an attractive method to assess spatial patterns of ecological impacts (e.g., Bierschenk et al., 2019; Mueller et al., 2020). Recently, also in hydropeaking rivers, such approaches are receiving increasing attention. However, so far, such studies only analyzed the interplay between hydropeaking and morphology (Schmutz et al., 2015) or natural environmental variables (Judes et al., 2020). To our

Table 4
Frequency of variable occurrence (total and per level) in the trees of the 69 single bootstrapping samples. Target variable: trichotomized grayling biomass.

Rank	Variable	Frequency ∑	Frequency ∑ per level				
			Level 1	Level 2	Level 3	Level 4	Level 5
1	MEFR_dW: mean downramping rate	80	65	7	6	2	0
2	CONN_2: habitat connectivity index 2	45	0	35	8	2	0
3	DUR: duration	34	0	12	15	4	3
4	CW: channel width index	22	0	6	11	4	1
5	CNT: yearly number of events	27	1	6	13	6	1
6	AMP_dW: peak amplitude	19	3	7	3	5	1
7	SSI: standard sinuosity index	11	0	1	5	4	1
8	POLL: biological assessment: pollutant load	4	0	1	2	0	1
9	SAP: saprobity baseline status	1	0	1	0	0	0

Table 5
Frequency of variable occurrence (total and per level) in the trees of the 69 single bootstrapping samples. Target variable: ecologically classified grayling biomass.

Rank	Variable	Frequency ∑	Frequency ∑ per level				
			Level 1	Level 2	Level 3	Level 4	Level 5
1	AMP_dW: peak amplitude	59	42	12	0	3	2
2	MEFR_dW: mean downramping rate	39	25	7	6	0	1
3	CNT: yearly number of events	39	1	22	14	2	0
4	CW: channel width index	37	1	21	10	4	1
5	SSI: standard sinuosity index	20	0	9	7	4	0
6	CONN_2: habitat connectivity index 2	19	0	1	13	5	0
7	DUR: duration	5	0	1	2	2	0

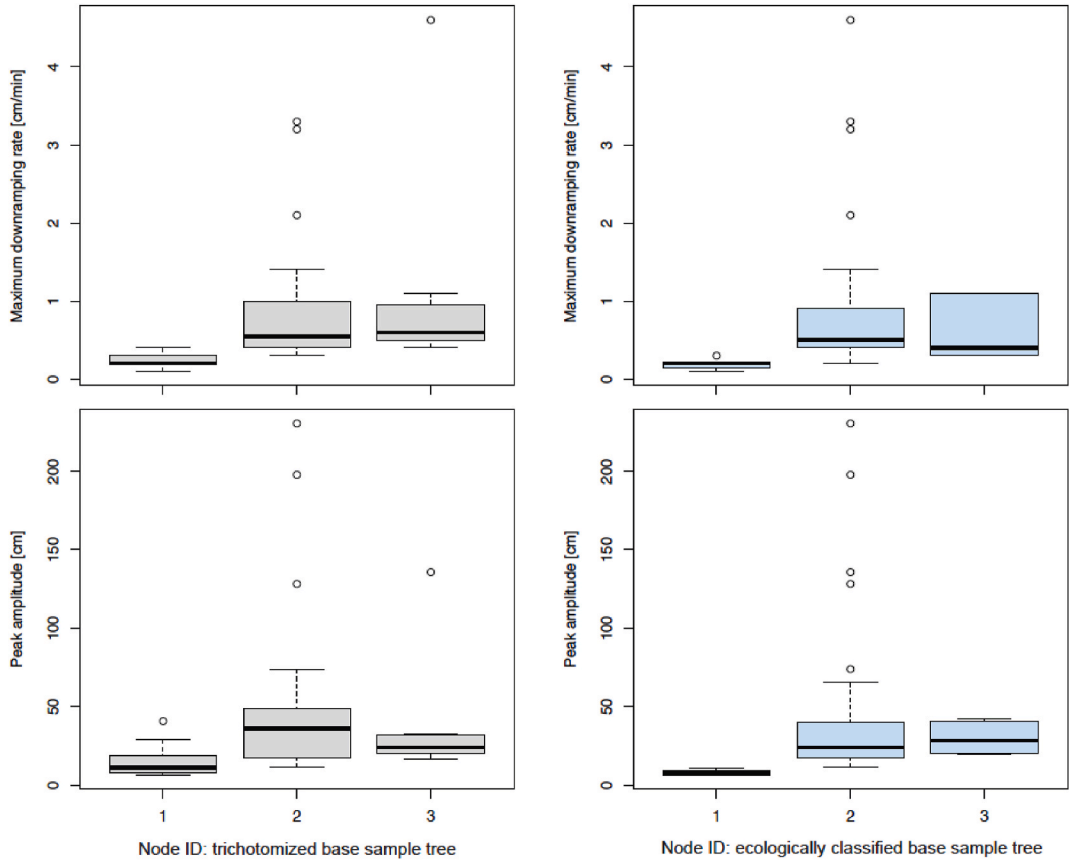

Fig. 5. Linking the end nodes of the base sample trees (Fig. 4) with maximum downramping rate and peak amplitude. See Figs. S4–S5 for boxplots with other hydropeaking variables. Boxplots: The boxes range from the first to the third quantile, the thick lines represent the median, and the bubbles are outliers (1.5 times the interquartile range).

knowledge, no study has yet conducted a large-scale comparison to analyze the effects of hydropeaking and further anthropogenic stressors on indicator fish populations of high conservational value, such as European grayling. Here, we filled this knowledge gap by identifying hydropeaking, fragmentation, and channelization as key stressors in hyporhithral rivers, thereby providing solid groundwork for river management decisions.

4.1. Hydropeaking mitigation thresholds

The coherence between the two tree models in the first level (Fig. 4) and the validation by the bootstrapping models strengthens the hypothesis that water level fluctuation is the primary driver in determining grayling population status. To derive operational management recommendations from the models, the end nodes have to be set within the context of other hydropeaking parameters as these are often highly correlated with each other (see Table S1). Based on node analyses with regards to selected hydropeaking parameters (Fig. 5, Figs. S4–S5), it can therefore be concluded that the critical peak amplitude range of artificial flow events lies between 10 and 25 cm, and the critical downramping velocity lies between 0.2 and 0.4 cm min^{-1}. Interestingly, the critical ramping range matches thresholds established for young-of-year grayling in experimental channels (Auer et al., 2014; Schmutz et al., 2013). Therefore, the fit between modelling and experimental approaches underlines the feasibility of using hydrological thresholds as ecological benchmarks for hydropeaking mitigation, particularly during critical life cycle stages such as fry emergence (Hayes et al., 2019; Moreira et al., 2019).

4.2. Hydromorphological criteria

In the second tree level, the models showed that, in hydropeaking rivers, high river network connectivity or heterogeneous habitat features can dampen the adverse effects of pulsed-flow releases (Fig. 4).

Regarding connectivity, the first model suggests that once a habitat complex >26 km is available, grayling populations can withstand hydropeaking impacts, at least to a certain degree (as the high biomass category is poorly represented in node 4). Considering that median home ranges are around 8 km (Junge et al., 2014) and migration distances range between 5 and 15 km (Jungwirth et al., 2000), this threshold seems reasonable from an ecological perspective. However, longer home ranges (>60 km) and migration distances (up to 100 km) have also been documented (Junge et al., 2014; Linløkken, 1993). Nevertheless, most home range studies include only adult fish and thus might underestimate the lifespan home range. Indeed, drift distances of grayling larvae alone can reach several kilometers (Meraner et al., 2013). Hence, this connectivity threshold must be interpreted with caution as a habitat network of 26 km might still be too small to sustain proper population sizes in many river systems, in particular, if key habitats are missing. In this regard, suitable spawning grounds and juvenile rearing areas are essential, and tributary connectivity probably plays a vital role in mitigating hydropeaking effects (Hauer et al., 2017).

As suggested by the second model, habitat quality is of equal importance to habitat quantity. Indeed, grayling require both, an intact river corridor and a heterogeneous morphology, to complete all life cycle stages (Jungwirth et al., 2000). It is well known that, in hydropeaking rivers, river bank morphology plays a key role in mitigating the impacts of flow regulation (Hauer et al., 2014; Moreira et al., 2019, 2020). Rivers with an array of sediment bars are most resilient to hydropeaking as they offer high habitat diversity in various flow conditions. Braided river reaches with flat and wide gravel bars, however, also exhibit a higher risk of fish stranding (Vanzo et al., 2016). In contrast, point bars show a low stranding risk (Hauer et al., 2014). Hence, based on modelling results, it has been suggested that transitional (i.e., between single-thread and multi-thread) river morphologies may offer best eco-hydraulic trade-offs between habitat diversity and stranding risk (Vanzo et al., 2016); however, field validations of this assumption are still vacant. Overall, at the population level, our results do not support the notion that nature-like hydropeaking rivers exhibit higher stranding risks than channelized ones.

Considering that the effects of morphology and connectivity are interaction effects, our findings also underline that the full benefits of river rehabilitation measures can only become visible if hydropeaking intensity is reduced at the same time. This conclusion is in line with other studies showing that hydropeaking can override the effects of morphological measures (Hellström et al., 2019; Muhar et al., 2007; Schmutz et al., 2015).

Water quality seems to play a negligibly role in Austrian hyporhithral rivers, as most sites exhibited a good status.

4.3. Shifting baselines?

Here, we used two approaches to transform the target variable into an ordinally-scaled variable. In an optimal case, with a more balanced distribution of sites, both would have yielded similar class widths. However, as grayling stocks throughout Europe have been in a continuous decline (e.g., Müller et al., 2018), it is increasingly difficult to acquire data from unimpacted sites. It is even likely that we are witnessing a shifting baseline of fish stocks. Hence, it was necessary to conduct analyses with both approaches. Surprisingly, however, both models not only showed a similar correct classification rate but, as discussed above, also yielded comparable results with regards to variable selection and splits.

4.4. Bootstrapping validation

The two bootstrapping approaches (Tables 4 and 5; Figs. S2-S3) confirmed that the original base sample sufficiently covers the main effects of levels 1–2. In the trichotomized version of the pooled sample, AMP_dW (≤25.5 cm) further split node 1 to separate higher and lower biomass sites (Figs. S2). This indicates that vital grayling populations depend upon low rates of various hydropeaking parameters.

To further distinguish hydropeaking-impacted sites, the trichotomized tree – as well as some of the single bootstrapped trees – selected DUR and CNT in level 3 (Fig. S2). Cases with longer peak duration yielded higher fish biomass than those with shorter duration. This pattern is expected as natural flow fluctuation events (e.g., floods) usually have a longer duration and lower mean downramping rate than hydropeaking events (Greimel et al., 2016). Regarding CNT, however, the direction of splits was somewhat unexpected: sites with a greater event frequency exhibited higher biomass than those with lower frequency. This pattern, which was also found in the ecologically classified tree (Fig. S3), can be partially explained by interpreting the bivariate relationship between fish biomass and event counts (Fig. S1): once the high biomass sites are cut off in the first tree level, the direction of the relationship seemingly reverses, leading to the presupposition that more hydropeaks produce higher biomass. Nevertheless, the seasonal timing of peaks may explain this pattern, which warrants further studies on the fish ecological effects of peak seasonality.

The ecologically classified tree also showed an unexpected split direction for CONN_2 in level 3 (Fig. S3), separating high biomass from medium biomass sites. A few high biomass sites are in sections shorter than ca. 10 km. This finding stresses the need to incorporate other measures such as (tributary) spawning grounds into future assessments (Hauer et al., 2017).

Both pooled bootstrapping trees selected river sinuosity (SSI) in some of their end nodes to separate higher biomass sites of more sinuous rivers from lower biomass sites in straight rivers (Figs. S2-S3). This pattern again showcases the importance of heterogeneous river channels for ecological integrity.

Summarizing, the pooled bootstrapping approach supported the base sample results and split the tree into deeper levels, thereby indicating which parameters are needed for future stressor assessments in hydropeaking rivers.

4.5. Limitations and research needs

A correct classification rate >70% and a high effect measure underline that the two variables chosen in each of the base sample trees were sufficient to predict grayling population status with high accuracy. Nevertheless, this also indicates that further factors may affect grayling, which were not covered in this study. For example, it has been suggested that piscivorous birds and anglers can diminish grayling stocks (Čech and Vejřík, 2011). Also, agricultural land-use may hamper this gravel-spawning species' reproduction if increased fine sediments loads infiltrate and clog gravel layers (Hauer et al., 2011; Müller et al., 2018), particularly if dams fail to release sediment-redistributing floods (Hayes et al., 2018). Furthermore, increasing water temperatures may not only limit the grayling's future habitat extent (Pletterbauer et al., 2016) but may already have contributed to recent abundance declines (Wedekind and Küng, 2010). Moreover, little is known about the population effects of food web changes, fish diseases, ubiquitous substances, or pharmaceutical products. Aside from multi-river studies on these topics, future research should focus on long-term assessments of case studies describing all ends of the pressure gradient. Such an approach would shed light on natural and anthropogenic effects and fulfill the requirements of an experiment from a statistical point of view.

5. Conclusions

Our results highlight the urgency of mitigating hydropeaking impacts to sustain or restore populations of threatened fish species such as European grayling. In this regard, the outcomes support the previously established notion of establishing ecologically-based flow thresholds (Moreira et al., 2019). Here, we identified critical ranges for peak amplitude (10–25 cm) and downramping velocity (0.2–0.4 cm min^{-1}) of

artificial flow events. Furthermore, this study underlines the need to maintain or re-establish river connectivity between morphologically diverse habitats to support the requirements of all life cycle stages of fish.

Credit author statement

Daniel S. Hayes: Conceptualization, Methodology, Formal analysis, Investigation, Data curation, Writing – original draft, Writing – review & editing, Visualization; Erwin Lautsch: Conceptualization, Methodology, Formal analysis, Writing – review & editing. Günther Unfer: Validation, Writing – review & editing. Franz Greimel: Data curation, Writing – review & editing. Bernhard Zeiringer: Validation, Writing – review & editing. Norbert Höller: Data curation. Stefan Schmutz: Conceptualization, Writing – review & editing, Supervision.

Data availability statement

Fish data is from: "Gewässerzustandsüberwachungsverordnung in Österreich gemäß Wasserrechtsgesetz 1959 idgF §§ 59 c-i bzw. Gewässerzustandsüberwachungsverordnung (GZÜV, BGBl II, 2006/479 idgF); BMNT, Abteilung I/3." All other data are available from corresponding author upon reasonable request.

Declaration of competing interest

The authors declare that they have no known competing financial interests or personal relationships that could have appeared to influence the work reported in this paper.

Acknowledgements

We are thankful for the support of Melanie Haslauer (fish data preparation), Martin Fuhrmann (input on the channel width index), Alex Piro (sinuosity index), and Carina Seliger (GIS-based Leitbild catalogue). CEF is a research unit funded by Fundação para a Ciência e a Tecnologia I.P. (FCT), Portugal (UID/AGR/00239/2013). DSH benefited from a Ph. D. grant sponsored by FCT (PD/BD/114440/2016).

Appendix A. Supplementary data

Supplementary data to this article can be found online at https://doi.org/10.1016/j.jenvman.2021.112737.

References

Auer, S., Fohler, N., Zeiringer, B., Führer, S., Schmutz, S., 2014. Experimentelle Untersuchungen zur Schwallproblematik. Drift und Stranden von Äschen und Bachforellen während der ersten Lebensstadien (Vienna).

Baudoin, J.-M., Burgun, V., Chanseau, M., Larinier, M., Ovidio, M., Sremski, W., Steinbach, P., Voegtle, B., 2015. Assessing the Passage of Obstacles by Fish. Concepts, Design and Application. ONEMA - Office National de l'Eau et des Milieux Aquatiques, Paris.

BAW, 2007. Fisch Index Austria (FIA) Leitbildkatalog.

Bierschenk, A.M., Mueller, M., Pander, J., Geist, J., 2019. Impact of catchment land use on fish community composition in the headwater areas of Elbe, Danube and Main. Sci. Total Environ. 652, 66–74. https://doi.org/10.1016/j.scitotenv.2018.10.218.

BMLFUW, 2017. Nationaler Gewässerbewirtschaftungsplan 2015 [National River Basin Management Plan 2015] (Vienna).

Braun, A., Auerswald, K., Geist, J., 2012. Drivers and spatio-temporal extent of hyporheic patch variation: implications for sampling. PloS One 7, e42046. https://doi.org/10.1371/journal.pone.0042046.

Breiman, L., Friedman, J.H., Olshen, R.A., Stone, C.J., 1984. Classification and Regression Trees. Chapman & Hall/CRC, New York.

Čech, M., Vejřík, L., 2011. Winter diet of great cormorant (Phalacrocorax carbo) on the River Vltava: estimate of size and species composition and potential for fish stock losses. Folia Zool. 60, 129–142.

DeLury, D.B., 1947. On the estimation of biological populations. Biometrics 3, 145–164.

Fuller, M.R., Doyle, M.W., Strayer, D.L., 2015. Causes and consequences of habitat fragmentation in river networks. Ann. N. Y. Acad. Sci. 1355, 31–51. https://doi.org/10.1111/nyas.12853.

Greimel, F., Schülting, L., Wolfram, G., Bondar-Kunze, E., Auer, S., Zeiringer, B., Hauer, C., 2018. Hydropeaking impacts and mitigation. In: Schmutz, S., Sendzimir, J. (Eds.), Riverine Ecosystem Management. Springer, pp. 91–110.

Greimel, F., Zeiringer, B., Hauer, C., Holzapfel, P., Fuhrmann, M., Haslauer, M., Führer, S., Höller, N., Grün, B., Habersack, H., Schmutz, S., 2017. Technischer Bericht B - Ökologische Bewertung schwalldämpfender Maßnahmen sowie weiterführende Analysen und Modelle (Vienna, Innsbruck).

Greimel, F., Zeiringer, B., Höller, N., Grün, B., Godina, R., Schmutz, S., 2016. A method to detect and characterize sub-daily flow fluctuations. Hydrol. Process. 30, 2063–2078. https://doi.org/10.1002/hyp.10773.

Grill, G., Lehner, B., Lumsdon, A.E., MacDonald, G.K., Zarfl, C., Liermann, C.R., 2015. An index-based framework for assessing patterns and trends in river fragmentation and flow regulation by global dams at multiple scales. Environ. Res. Lett. 10, 015001.

Harrison, P.M., Martins, E.G., Algera, D.A., Rytwinski, T., Mossop, B., Leake, A.J., Power, M., Cooke, S.J., 2019. Turbine entrainment and passage of potadromous fish through hydropower dams: developing conceptual frameworks and metrics for moving beyond turbine passage mortality. Fish Fish. 20, 403–418. https://doi.org/10.1111/faf.12349.

Hauer, C., Holzapfel, P., Leitner, P., Graf, W., 2017. Longitudinal assessment of hydropeaking impacts on various scales for an improved process understanding and the design of mitigation measures. Sci. Total Environ. 575, 1503–1514. https://doi.org/10.1016/j.scitotenv.2016.10.031.

Hauer, C., Unfer, G., Holzapfel, P., Haimann, M., Habersack, H., 2014. Impact of channel bar form and grain size variability on estimated stranding risk of juvenile brown trout during hydropeaking. Earth Surf. Process. Landforms 39, 1622–1641. https://doi.org/10.1002/esp.3552.

Hauer, C., Unfer, G., Tritthart, M., Habersack, H., 2011. Effects of stream channel morphology, transport processes and effective discharge on salmonid spawning habitats. Earth Surf. Process. Landforms 36, 672–685. https://doi.org/10.1002/esp.2087.

Haunschmid, R., Honsig-Erlenburg, W., Petz-Glechner, R., Schmutz, S., Schotzko, N., Spindler, T., Unfer, G., Wolfram, G., 2006. Methodik – Handbuch, Fischbestandsaufnahmen in Fließgewässern. Scharfling.

Hayes, D.S., Brändle, J.M., Seliger, C., Zeiringer, B., Ferreira, T., Schmutz, S., 2018. Advancing towards functional environmental flows for temperate floodplain rivers. Sci. Total Environ. 633, 1089–1104. https://doi.org/10.1016/j.scitotenv.2018.03.221.

Hayes, D.S., Moreira, M., Boavida, I., Haslauer, M., Unfer, G., Zeiringer, B., Greimel, F., Auer, S., Ferreira, T., Schmutz, S., 2019. Life stage-specific hydropeaking flow rules. Sustainability 11, 1547. https://doi.org/10.3390/su11061547.

Hellström, G., Palm, D., Brodin, T., Rivinoja, P., Carlstein, M., 2019. Effects of boulder addition on European grayling (Thymallus thymallus) in a channelized river in Sweden. J. Freshw. Ecol. 34, 559–573. https://doi.org/10.1080/02705060.2019.1614102.

Horacio, J., 2014. River Sinuosity Index: Geomorphological Classification.

Huet, M., 1959. Profiles and biology of western European streams as related to fish management. Trans. Am. Fish. Soc. 88, 155–163. https://doi.org/10.1577/1548-8659(1959)88[155:PABOWE]2.0.CO;2.

IBM Statistics, 2016. IBM SPSS Statistics 24 Algorithms.

Judes, C., Gouraud, V., Capra, H., Maire, A., Barillier, A., Lamouroux, N., 2020. Consistent but secondary influence of hydropeaking on stream fish assemblages in space and time. J. Ecohydraulics. https://doi.org/10.1080/24705357.2020.1790047.

Junge, C., Museth, J., Hindar, K., Kraabøl, M., Vøllestad, A.L., 2014. Assessing the consequences of habitat fragmentation for two migratory salmonid fishes. Aquat. Conserv. Mar. Freshw. Ecosyst. 24, 297–311. https://doi.org/10.1002/aqc.2391.

Jungwirth, M., Muhar, S., Schmutz, S., 2000. Fundamentals of fish ecological integrity and their relation to the extended serial discontinuity concept. Hydrobiologia 422/423, 85–97.

Linløkken, A., 1993. Efficiency of fishways and impact of dams on the migration of grayling and brown trout in the Glomma river system, south-eastern Norway. Regul. Rivers Res. Manag. 8, 145–153. https://doi.org/10.1002/rrr.3450080117.

Meraner, A., Unfer, G., Gandolfi, A., 2013. Good news for conservation: mitochondrial and microsatellite DNA data detect limited genetic signatures of inter-basin fish transfer in Thymallus thymallus (Salmonidae) from the Upper Drava River. Knowl. Manag. Aquat. Ecosyst. 409 https://doi.org/10.1051/kmae/2013046.

Moreira, M., Hayes, D.S., Boavida, I., Schletterer, M., Schmutz, S., Pinheiro, A., 2019. Ecologically-based criteria for hydropeaking mitigation: a review. Sci. Total Environ. 657, 1508–1522. https://doi.org/10.1016/j.scitotenv.2018.12.107.

Moreira, M., Schletterer, M., Quaresma, A., Boavida, I., Pinheiro, A., 2020. New insights into hydropeaking mitigation assessment from a diversion hydropower plant: the GKI project (Tyrol, Austria). Ecol. Eng. 158, 106035. https://doi.org/10.1016/j.ecoleng.2020.106035.

Mueller, M., Bierschenk, A.M., Bierschenk, B.M., Pander, J., Geist, J., 2020. Effects of multiple stressors on the distribution of fish communities in 203 headwater streams of Rhine, Elbe and Danube. Sci. Total Environ. 703, 134523. https://doi.org/10.1016/j.scitotenv.2019.134523.

Muhar, S., Jungwirth, M., Unfer, G., Wiesner, C., Poppe, M., Schmutz, S., Hohensinner, S., Habersack, H., 2007. 30 Restoring riverine landscapes at the Drau River: successes and deficits in the context of ecological integrity. Dev. Earth Surf. Process 11, 779–803. https://doi.org/10.1016/S0928-2025(07)11164-0.

Muhar, S., Schwarz, M., Schmutz, S., Jungwirth, M., 2000. Identification of rivers with high and good habitat quality: methodological approach and applications in Austria. Hydrobiologia 422/423, 343–358.

Muhar, S., Seliger, C., Schinegger, R., Scheikl, S., Brändle, J., Hayes, D.S., Schmutz, S., 2019. Status and protection of rivers. A pan-Alpine overview. In: Muhar, Susanna,

Muhar, A., Egger, G., Siegrist, D. (Eds.), Rivers of the Alps. Diversity in Nature and Culture. Haupt, Berne, pp. 302–319.

Müller, M., Pander, J., Geist, J., 2018. Comprehensive analysis of >30 years of data on stream fish population trends and conservation status in Bavaria, Germany. Biol. Conserv. 226, 311–320. https://doi.org/10.1016/j.biocon.2018.08.006.

National Research Council, 1988. The Behavioral and Social Sciences: Achievements and Opportunities. The National Academies Press, Washington, DC. https://doi.org/10.17226/992.

Nykänen, M., 2004. Habitat Selection by Riverine Grayling, Thymallus thymallus L. University of Jyväskylä.

Pletterbauer, F., Graf, W., Schmutz, S., 2016. Effect of biotic dependencies in species distribution models: the future distribution of Thymallus thymallus under consideration of Allogamus auricollis. Ecol. Model. 327, 95–104. https://doi.org/10.1016/j.ecolmodel.2016.01.010.

Schinegger, R., Trautwein, C., Melcher, A., Schmutz, S., 2012. Multiple human pressures and their spatial patterns in European running waters. Water Environ. J. 26, 261–273. https://doi.org/10.1111/j.1747-6593.2011.00285.x.

Schmutz, S., Bakken, T.H., Friedrich, T., Greimel, F., Harby, A., Jungwirth, M., Melcher, A., Unfer, G., Zeiringer, B., 2015. Response of fish communities to hydrological and morphological alterations in hydropeaking rivers of Austria. River Res. Appl. 31, 919–930. https://doi.org/10.1002/rra.2795.

Schmutz, S., Fohler, N., Friedrich, T., Fuhrmann, M., Graf, W., Greimel, F., Höller, N., Jungwirth, M., Leitner, P., Moog, O., Melcher, A., Müllner, K., Ochsenhofer, G., Salcher, G., Steidl, C., Unfer, G., Zeiringer, B., 2013. Schwallproblematik an Österreichs Fließgewässern – Ökologische Folgen und Sanierungsmöglichkeiten (Vienna).

Schmutz, S., Zauner, G., Eberstaller, J., Jungwirth, M., 2001. Die "Streifenbefischungsmethode": eine Methode zur Quantifizierung von Fischbeständen mittelgroßer Fließgewässer. Österreichs Fischerei 54, 14–27.

Seber, G.A.F., Le Cren, E.D., 1967. Estimating population parameters from catches large relative to the population. J. Anim. Ecol. 36, 631–643.

Sempeski, P., Gaudin, P., 1995. Size-related changes in diel distribution of young grayling (Thymallus thymallus). Can. J. Fish. Aquat. Sci. 52, 1842–1848.

Silva, A.T., Lucas, M.C., Castro-Santos, T., Katopodis, C., Baumgartner, L.J., Thiem, J.D., Aarestrup, K., Pompeu, P.S., O'Brien, G.C., Braun, D.C., Burnett, N.J., Zhu, D.Z., Fjeldstad, H.-P., Forseth, T., Rajaratnam, N., Williams, J.G., Cooke, S.J., 2018. The future of fish passage science, engineering, and practice. Fish Fish. 19, 340–362. https://doi.org/10.1111/faf.12258.

Stubauer, I., Moog, O., 2003. Saprobielle Grundzustände Österreichischer Fließgewässer (Vienna).

Vannote, R.L., Minshall, G.W., Cummins, K.W., Sedell, J.R., Cushing, C.E., 1980. The river continuum concept. Can. J. Fish. Aquat. Sci. 37, 130–137. https://doi.org/10.1139/f80-017.

Vanzo, D., Zolezzi, G., Siviglia, A., 2016. Eco-hydraulic modelling of the interactions between hydropeaking and river morphology. Ecohydrology 9, 421–437. https://doi.org/10.1002/eco.1647.

Von Eye, A., 2002. Configural Frequency Analysis: Methods, Models, and Applications. Lawrence Erlbaum Associates, Inc., Mahwah, NJ.

Von Eye, A., Mair, P., Mun, E.Y., 2010. Advances in Configural Frequency Analysis. Guilford Press, New York.

Wedekind, C., Küng, C., 2010. Shift of spawning season and effects of climate warming on developmental stages of a grayling (salmonidae). Conserv. Biol. 24, 1418–1423. https://doi.org/10.1111/j.1523-1739.2010.01534.x.